Three-Dimensional Finite-Element Analysis of Pressure–Settlement Response of Sand Compaction Pile-Treated Cohesionless Deposits

Article *in* International Journal of Geomechanics · April 2021

DOI: 10.1061/(ASCE)GM.1943-5622.0001957

2 authors:

Aarthi Natrajan
Indian Institute of Technology Madras
2 PUBLICATIONS **2** CITATIONS
SEE PROFILE

G. R. Dodagoudar
Indian Institute of Technology Madras
123 PUBLICATIONS **1,178** CITATIONS
SEE PROFILE

Three-Dimensional Finite-Element Analysis of Pressure–Settlement Response of Sand Compaction Pile-Treated Cohesionless Deposits

N. Aarthi[1] and G. R. Dodagoudar[2]

Abstract: Strength characteristics of loose to medium dense sand deposits improved by sand compaction piles (SCPs) are assessed by performing three-dimensional (3D) finite-element analysis using PLAXIS 3D. The Mohr–Coulomb model is employed to model the behavior of both sand and SCP. A laboratory test is performed on the SCP-treated sand deposit to validate the finite-element (FE) result and they are in good agreement. A parametric study is conducted on field-scale SCP FE models considering variations in the properties of sand deposit and geometrical parameters of the SCP on the pressure–settlement response. Based on the FE results, it is found that a nearly 21% increment in the ultimate bearing capacity of the SCP-treated sand deposit can be obtained when the diameter of the SCP is increased by 100 mm. Settlement improvement factors are estimated for the treated sand deposits at selected bearing pressures to understand the extent of improvement achieved. **DOI: 10.1061/(ASCE)GM.1943-5622.0001957**. *© 2021 American Society of Civil Engineers*.

Author keywords: Sand deposit; PLAXIS 3D; Pressure–settlement response; SCP method.

Introduction

Rapid urbanization and infrastructure development increases the need for tremendous growth in the construction sector in India. Therefore, the natural grounds comprising weak soil deposits have to be treated with various ground improvement techniques to transfer the load safely from the superstructure to the ground underneath. Loose sands, marine clays, and expansive clays are the commonly found problematic soils in India (Uppal and Chadda 1967; Singh et al. 2005; Basack and Purkayastha 2009; Dixit 2016). Kankara et al. (2018) stated in an NCCR (National Centre for Coastal Research, India) report that 43% of the Indian coastline contains cohesionless deposits. Construction of structures such as harbors, dry docks, jetties, and other related infrastructure facilities is inevitable in these coastlines exceeding 6,500 km. These deposits are often present in loose to medium dense conditions and therefore need improvement before undertaking any type of construction activity. Techniques such as dynamic compaction, blasting, installation of columnar inclusions [e.g., stone columns, sand compaction piles (SCPs)] can be used to enhance the engineering properties of the natural loose sand deposits present at the site, IS:13094 (BIS 1992).

Several researchers demonstrated the importance of understanding the strength characteristics of stone columns in soft soils by conducting laboratory and field tests (Ambily and Gandhi 2007; Yi et al. 2013; Bouassida and Carter 2014; Takeuchi et al. 2010; Jeludin et al. 2016; Basack et al. 2018). A contemporary technique to the stone columns is the SCP method, which was developed in Japan in 1956. The principle of this ground improvement method is based on the displacement of the original loose deposit by installing sand piles, thereby densifying the ground (Kitazume et al. 2016). The widespread implementation of the SCP method is deployed at Kansai International Airport in Japan (Aboshi et al. 1979), Marina Bay in Singapore (Wei 1997), and Pipavav Shipyard in Gujarat, India (Raj and Dikshith 2010).

The field procedure implementation of the SCP technique goes by the following protocol: (1) measuring initial standard penetration test (SPT-N) value, (2) finding the liquefaction potential, (3) install SCP to reduce the liquefaction susceptibility by fixing the target SPT-N value—to enhance the strength characteristics and liquefaction resistance (Moh et al. 1981; Yasuda et al. 1996; Kinoshita et al. 2012). Several studies available in the literature as aforementioned focused on the versatility of the SCP technique in mitigating liquefaction hazards. Very few works of literature stated the importance of studying the strength characteristics of the granular column-improved cohesionless deposits from a pressure–settlement perspective (Samanta et al. 2010; Aarthi et al. 2019). In a cohesionless deposit reinforced by SCPs, the parameters that affect the performance significantly are as follows: diameter and spacing of SCPs, strength parameters of the intervening soil, and the pile material (Ashwathy et al. 2013). Limited studies in the past have reported the significance of parameters such as initial relative density (RD) (Hatanaka et al. 2008) and the number of SCPs (Samanta et al. 2010) in improving the performance of cohesionless deposits.

Although the SCP technique is widely implemented in South-East Asian countries, the independent strength characteristics of the treated ground devoid of liquefaction resistance perspective were not studied in detail. Also, comprehensive studies on the major parameters affecting the SCP-treated sandy grounds and their role in altering the bearing capacity after the improvement have not been given enough importance in the literature. A clear understanding of the pressure–settlement characteristics of the

[1]Assistant Professor, Dept. of Civil Engineering, KPR Institute of Engineering and Technology, Coimbatore; formerly, Doctoral Research Fellow, Dept. of Civil Engineering, Indian Institute of Technology Madras, Chennai 600036, India (corresponding author). ORCID: https://orcid.org/0000-0001-5824-0080. Email: aarthicivilian@gmail.com

[2]Professor, Computational Geomechanics Laboratory, Dept. of Civil Engineering, Indian Institute of Technology Madras, Chennai 600036, India.

Note. This manuscript was submitted on April 21, 2020; approved on October 23, 2020; published online on January 20, 2021. Discussion period open until June 20, 2021; separate discussions must be submitted for individual papers. This paper is part of the ***International Journal of Geomechanics***, © ASCE, ISSN 1532-3641.

SCP-improved cohesionless deposits could provide great help for more effective implementation of the technique.

Therefore, the present study is aimed at addressing the effect of initial RD, diameter and length of SCP, and spacing on the pressure–settlement response of the SCP-treated sand deposits by three-dimensional (3D) FE simulations. Laboratory load tests are performed on the SCP-treated sandbed to validate the FE results. Then, the 3D FE simulations are performed on the field-scale SCP-treated sand deposit considering variations in the initial RD of the sand deposit, diameter (D) and length (L) of the SCP, and spacing (S) between the SCPs on the pressure–settlement response under static compressive loads.

FE Simulation of Lab-Scale Response of SCP-Improved Deposit

The FE simulations are performed using PLAXIS 3D 2013.01 (Vermeer and Brinkgreve 2013); hereafter, it is referred to as PLAXIS 3D for the evaluation of the pressure–settlement response of the SCP-treated sand deposit. The procedure to perform finite-element analysis (FEA) with PLAXIS is: the creation of a problem domain, assigning boundary conditions, choosing material model, assigning input properties, simulation of SCP installation, discretization, calculation of initial stresses, defining and executing stage-wise phase calculations, obtaining the output, and evaluation of results.

FE Domain and Boundary Conditions

The FE domain created is of dimension 1,000 × 1,000 × 850 mm to represent the test tank (Fig. 1). The testbed is simulated by considering the dimensions as adopted in the laboratory experiment. The sand volume is introduced into the FE domain by using the *borehole option* available in the software. PLAXIS 3D by default imposes a set of general fixities to the boundaries of the FE domain and if needed; these general fixities can be controlled during the stage-wise computations. For the present FE simulation, the top surface is set free in all directions and the bottom layer is fixed in all directions, i.e., $U_x = U_y = U_z = 0$. The xz- and yz-planes are set free to move up to a prescribed displacement of 80 mm in the z-direction (Fig. 5). The laboratory test setup is depicted in Fig. 1 and the same is simulated in PLAXIS.

Material Model and Input Properties

Among the material models of PLAXIS 3D, the Mohr–Coulomb (MC) and hardening soil (HS) models are found to be adequate to characterize the behavior of the cohesionless deposits (Carter et al. 2000; Damians et al. 2015). The HS model is appropriate to model the strain-hardening behavior of sands and is preferred only in specific applications where the unloading behavior is of primary focus (e.g., excavation related problems). Moreover, sophisticated monitoring is required to obtain the input properties required for the HS model (Jozefiak et al. 2015). The MC model can be applied to several problems such as cavity expansion, embankment stability, and evaluation of bearing capacity of footing as reported by Coombs et al. (2013). The objective of the present study is to evaluate the ultimate bearing capacity (UBC) of the SCP-treated ground. Therefore, the MC material model is used instead of the HS model to simulate the pressure–settlement response of the SCP-treated sandbed. The MC model has been used extensively for the analysis of many geotechnical problems (Savidis et al. 2008; Lozovyi and Zahouriko 2012; Hanna et al. 2013; Bhowmik and Samanta 2013). The loose

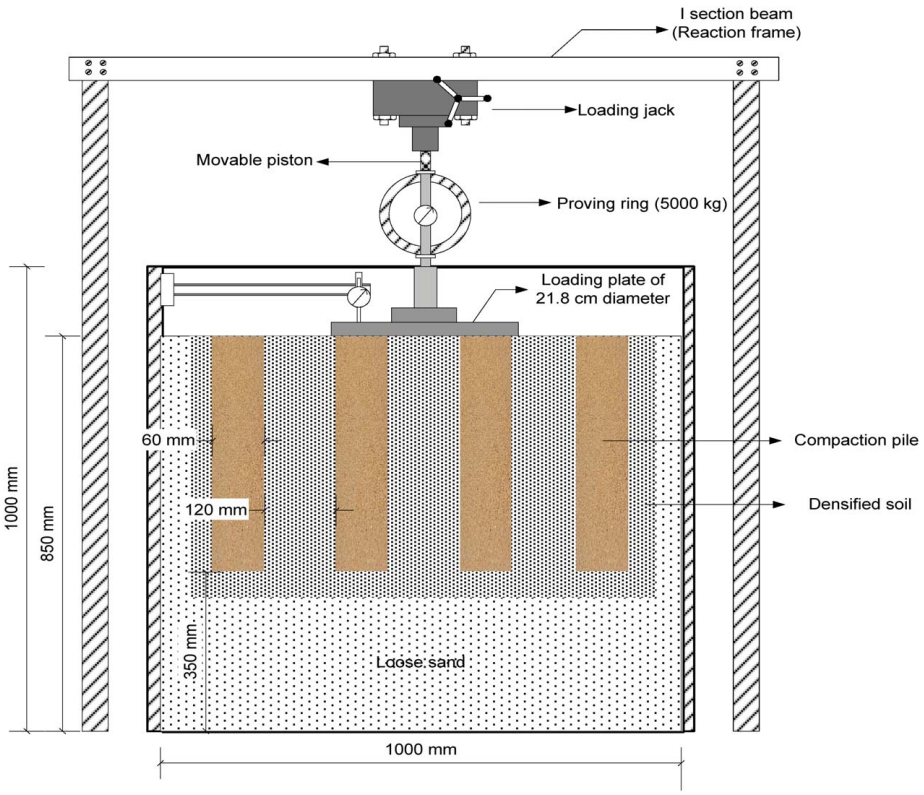

Fig. 1. Schematic of plate load test setup for the SCP group.

Int. J. Geomech., 2021, 21(4): 04021019

Table 1. Soil properties for FE lab-scale model

Properties	γ (kN/m^3)	E (MPa)	υ	ϕ	R_{inter}
Tank sand	16.4	35	0.25	32	0.9
SCP	17.3	45	0.3	39	0.9

sand is used as the initial medium and the corresponding input properties are given in Table 1.

The angle of internal friction (ϕ) of the sand is determined by ASTM D3080/D3080M-11 (ASTM 2011). The properties of the SCPs simulated pertain to the sand with an RD of 73%. The unit weight of the treated sand is obtained using correlation relating to the RD measured after the installation of the SCPs. The dilation angle (ψ) is calculated using Eq. (1), as recommended by Bolton (1986):

$$\psi = \theta - 30^\circ \tag{1}$$

The dilation angles employed in the current study vary from 1° to 9°, which lies in good agreement with the range of dilation angles for pure sands reported by Madhusudhan et al. (2019). Poisson's ratio is adopted from typical values suggested by Bowles (1996). Young's modulus of the sand is obtained using Eq. (2) where the SPT-N value corresponds to the RD of the treated sandbed (Bowles 1996):

$$E = 7{,}000\sqrt{N} \tag{2}$$

R_{inter} = interface strength reduction factor between the plate and the sand beneath it. This defines the percentage of friction mobilized at the interface to produce the deformation. An R_{inter} of 0.9 is used in the modeling, which lies within the range reported by Damians et al. (2015).

Simulation of SCP Installation

To simulate the response of pile realistically, the increase of stresses due to installation has to be simulated reasonably well in the numerical analysis. Broere and van Tol (2006) reported that the complex interactions associated with the aforementioned problem were not handled properly and there was not much progress in the FE modeling of the displacement piles. Since then, several procedures have been developed to simulate the pile installation process, thereby accounting for the increase of stresses caused by the driven piles in the numerical simulations (Hurley et al. 2015; Kranthikumar et al. 2016; Ammari and Clarke 2018). The aforementioned studies used PLAXIS to accommodate the large strain deformation responses associated with the installation of a displacement pile.

In the present study, the installation of SCP of diameter 60 mm and length 500 mm is accomplished in the sandbed by applying the volumetric strain based on the principle of cavity expansion at the location of the SCP in the FE domain. This way of installation densifies the sandbed by displacing the sand laterally away from the SCP. The volumetric strain due to SCP installation in the cohesionless deposit is equal to that of the area replacement ratios (ARR) adopted (Yamamoto et al. 1997; Nyström and Persson 2016). The volumetric strains of 6% and 11% have been observed in the sand deposits during pile installations (White and Bolton 2002; Hatanaka et al. 2008), where higher volumetric strains correspond to higher RD and higher drained strength. After installation, any discrepancies in the field measurements of the increased density can be due to ground heave and excessive lateral deformation of the deposit treated using the SCPs (Harada et al. 1998). The volumetric strain adopted in the present lab-scale FE modeling is 12%, which is the ARR adopted in the laboratory test for the 2D spacing.

Laboratory Experiment: SCP-Treated Sandbed

The small-scale laboratory plate load test on the SCP group with 2 and 2.5D spacing involves the sandbed prepared at 40% initial RD. The footing (made up of mild steel, diameter = 218 mm for 2D and 273 mm for 2.5D) resting over the three numbers of SCP, in the treated sandbed was subjected to static compressive load and the pressure–settlement response was obtained. The test was conducted until the settlement reached a maximum value of 80 mm. It was observed that with an increase in the load, the settlement of the footing continued to increase. And after a particular instance, with only a marginal increase in the load, the settlement continued to increase indicating the failure of the SCP-treated sandbed. The results of the load tests are presented in the form of pressure–settlement response (Fig. 3). In the present study, the UBC is estimated by using the double tangent method (Aarthi et al. 2019).

FE Simulation and Validation

The diameter of the footing is calculated using the unit cell approach (Han 2015) and it covers the surface area of the three SCPs, along with their tributary areas. The footing is modeled using linear-elastic plate elements with the properties of the mild steel: thickness = 8 mm, unit weight = 75.5 kN/m^3, Poisson's ratio = 0.33, and Young's modulus = 200 GPa. For discretization, a few trial sensitivity analyses are performed using different mesh sizes. The convergence of the FE model is achieved for the medium meshing with a relative element size factor, $r_e = 1$. The entire soil medium and the SCPs are discretized into 10-node tetrahedral elements. The *plastic analysis* option available in the solution techniques of the PLAXIS is used for the stage-wise calculations. Loading over the footing is applied in terms of prescribed displacement of 80 mm incrementally.

The reasoning behind choosing an 80 mm settlement value is as follows: the load tests on the SCP-treated sandbed in the laboratory were carried out based on the procedure recommended by ASTM D1196/D96M-12 (ASTM 2016). The tests were continued until the settlement reached a maximum value of 80 mm and the same value is used as prescribed displacements in the FE simulations. This settlement value was selected to capture the complete load–settlement response and failure strains for the medium dense sand condition. The same reason is also applicable for choosing 0.1 m prescribed displacement value for field-scale FE models.

The deformed FE mesh for the laboratory setup of the SCP group is depicted in Fig. 2. The pressure–settlement response is obtained at the bottom (i.e., at the center) of the footing having coordinates (500, 500). The result of the FE analysis is compared with the experimental result and is found to be in good agreement with a reasonable match between them, as shown in Fig. 3. It can be noticed that the output from the FE model of 2D spacing sustained a full displacement of 80 mm. However, the FE model of 2.5D spacing failed at 65 mm of displacement, as depicted in Fig. 3. Thereby, it can be stated that PLAXIS is capable of simulating the pressure–settlement behavior of the SCP-treated sand deposits. The heaving of the SCP-improved sandbed around the footing is visible in Fig. 2. It can be noticed that the heaving of the SCP-treated sand deposits is a common occurrence in field applications as well (Yabushita et al. 1973; Sogabe 1981; Hirao and Matsuo 1985; Shiomi and Kawamoto 1986).

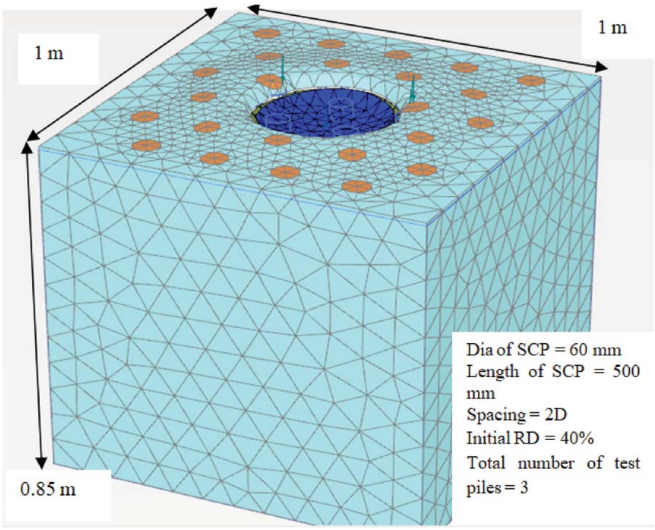

Fig. 2. Deformed FE mesh for the laboratory setup of the SCP group (initial RD = 40%, $S = 2D$).

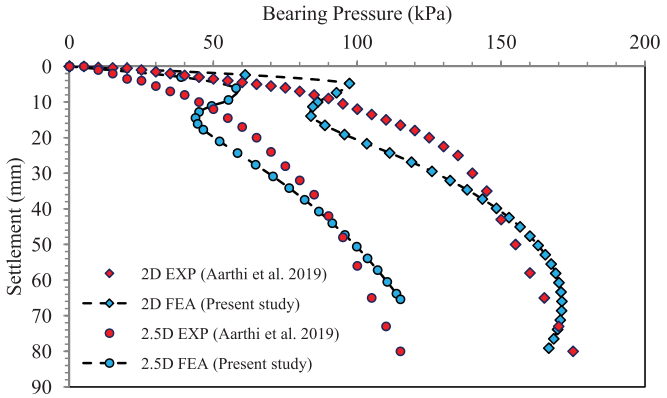

Fig. 3. Comparison of the pressure–settlement response of the SCP-improved sandbed (40% initial RD, 2*D*, and 2.5*D* spacing): FE and laboratory results.

FE Simulation of Field-Scale Problem of the SCP-Improved Ground

The laboratory-scale FE model developed aforementioned is extended to the field dimensions of 25 × 25 × 25 m soil domain to evaluate the behavior of SCP-improved loose to medium dense sand deposits. Three SCP group is driven to a depth of 20 m from the ground level in the loose sand deposit of initial RD = 30% and spacing of 2*D*. Along with the SCP group to be loaded, the sand deposit surrounding the group is treated with one layer of SCP (i.e., nine SCPs) similar to the field conditions. The load is applied in the form of a prescribed displacement of 0.1 m on the footing, whose surface area is approximately equal to three times the effective diameter of the SCPs. The input properties of the installed SCPs correspond to an RD of 73%. The material and geometric parameters used in the FE simulations of the field-scale SCP model are presented in Tables 2 and 3. This section considers only the simulation of the base FE model having the following parameters: initial RD = 30%, diameter and length of SCP = 0.6 and 20 m, spacing = 2*D*, and other properties, as given in Table 3.

Fig. 4 depicts the deformation pattern obtained after installation of the SCPs by PLAXIS using the cavity expansion theory

Table 2. Range of parameters used in FE simulations

Parameter	Range
Initial relative density (%)	30, 40, 50, 60
Diameter of SCP (m)	0.5, 0.6, 0.7, 0.8
Length of SCP (m)	5, 10, 15, 20
Spacing/diameter (*S*/*D*) ratio	1.5, 2, 2.5, 3, 3.5

Table 3. Input properties of sand deposit and SCP used in the parametric studies

Description	Parameter	Value	Unit	Range
Sand deposit	Γ	16.4	kN/m^3	16.4–16.7
	E	35	MPa	35, 36, 37, 38
	ν	0.25	—	0.25–0.3
	ϕ	32	—	32, 33, 34, 35
	ψ	2		2, 3, 4, 5
	R_{inter}	0.9	—	—
SCP	Γ	17.3	kN/m^3	—
	E	45	MPa	—
	ν	0.3	—	—
	ϕ, ψ	39, 9	—	—
	R_{inter}	0.9	—	—

in the sand deposit of the initial RD = 30%. Based on the ARR, for the present model, a total volumetric strain of 6% is applied at the respective locations of the SCPs to simulate the installation, which displaces the sand along the pile shaft for the entire length of the SCP. This way of installation of the SCPs in the numerical model simulates the field procedure. Fig. 5 shows the sectional view at the center of the FE model depicting the mesh discretization of the soil domain and the installed SCP cluster at the center of the deposit. The prescribed displacement of 0.1 m is applied on the footing and the pressure–settlement response of the improved deposit is obtained. Fig. 6 shows the closer view of the FE model surrounding the group depicting the applied prescribed displacement. The pressure–settlement response (Fig. 7) is obtained at the center node of the FE domain below the footing (12.5, 12.5, and 0 m).

With the properties of the sand deposit and SCP remaining the same in the laboratory- and field-scale base models, the field-scale model is simulated with the following scale factors expressed in a ratio of laboratory FE model to field-scale FE model: dimensions of FE domain (1/25), footing diameter (1/10), SCP diameter (1/10), and SCP length (1/40). Past studies on the scale effects of foundations in reinforced soils reveal that the load–settlement response of reinforced soil is not sensitive to the scale effect if the settlement (s) is expressed in a nondimensional relative settlement of s/d, where d is the diameter of the footing (Briaud and Gibbens 1994; Fellenius and Altaee 1994; Chen and Farsakh 2011).

Initial in situ stresses are calculated separately during the initial phase of calculations and are considered in the stage-wise phase calculations, default by the software. The SCPs are installed in the next phase, where the displacements caused due to the installation of SCP is accommodated in the FE modeling at this phase itself. The prescribed displacement of 0.1 m for simulating the static compression loading is applied only at the final phase of the stage-wise calculations in the FE modeling.

Parametric Sensitivity Analyses: 3D FE Results

The influence of parameters, namely, initial RD of the sand deposit, diameter and length of SCP, the spacing between

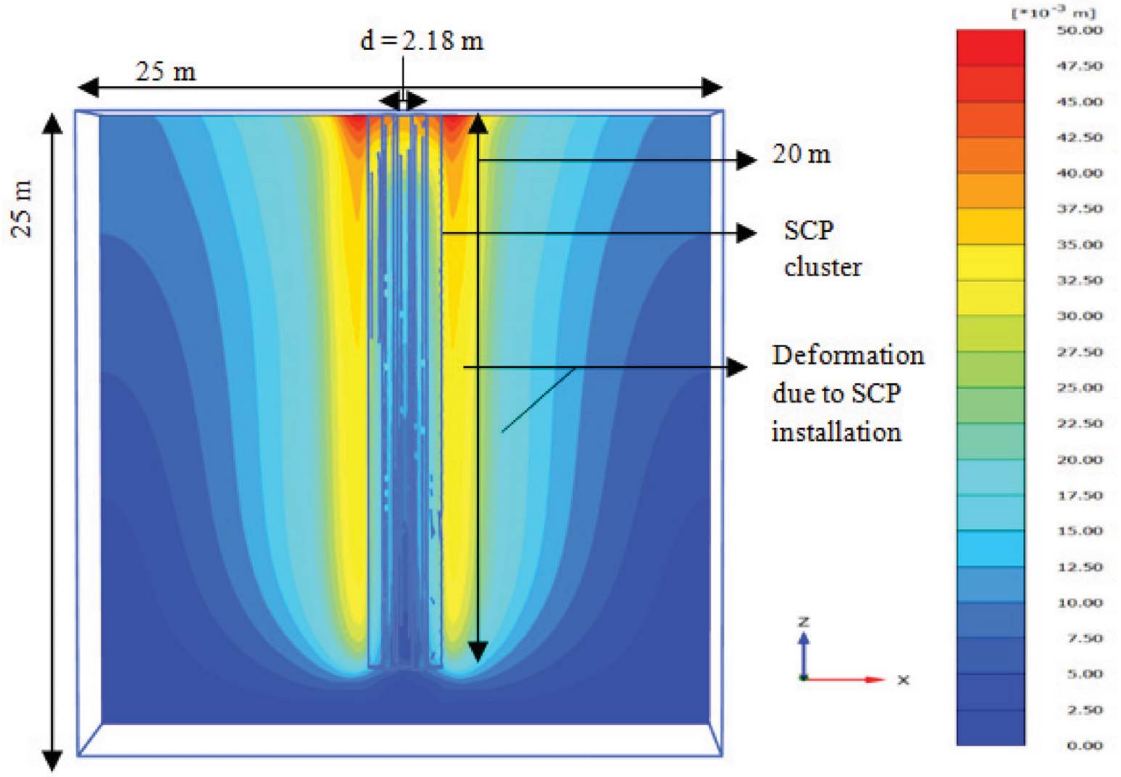

Fig. 4. Deformation pattern in the sand deposit after installation of SCPs.

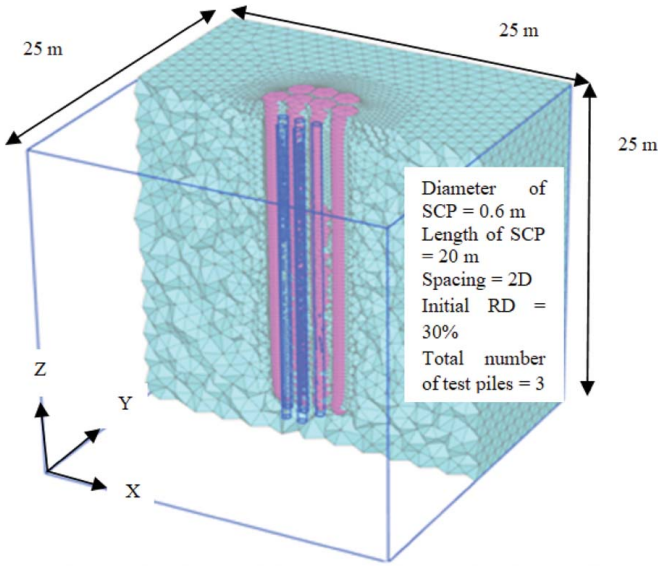

Fig. 5. Sectional view of the FE domain with a cluster of the installed SCPs.

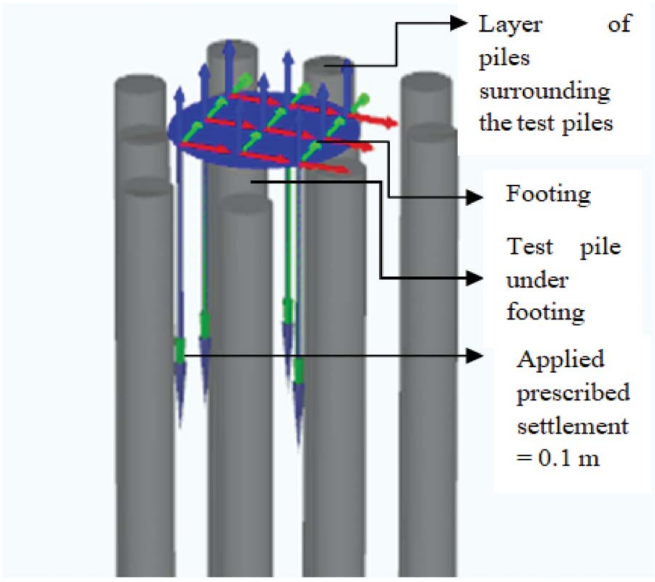

Fig. 6. Close view of the SCP group showing prescribed displacement (base model: initial RD = 30%, $D = 0.6$ m, $L = 20$ m, $S = 2D$).

the SCPs on the pressure–settlement response, and settlement improvement factor (SIF) of the improved deposit is discussed in this section. The parametric study is carried out on the 3D field-scale model for the selected range of geometrical parameters of the SCPs and the initial RD of the sand deposit, as given in Table 2. All the FE simulations for the field-scale SCP problem are performed for the prescribed total displacement of 0.1 m on the footing supported on the three numbers of compaction piles.

Effect of Initial RD of the Surrounding Sand Deposit

In this section, the initial RDs of the sand deposit will only take different values in the FE analysis (i.e., 30%–60%). The other parameters, namely, diameter and length of the SCP = 0.6 and 20 m, and spacing = $2D$ are kept constant. Fig. 7 depicts the pressure–settlement behavior of the treated sand deposit for the aforementioned parametric combinations. The trend obtained from the FEA for the field-scale problem is similar to that obtained from

the experimental result. The response obtained for the untreated sand deposit of initial RD = 30% is also shown in Fig. 7 to understand the extent of improvement achieved by the SCP installation. The pressure–settlement plots of the treated deposit contain two distinct parts: the initial linear one independent of the RDs considered, the second one wherein the SCP-improved deposit undergoes plastic deformation differing from each other pertaining to the different initial RDs of the deposit. The pressure–settlement plots corresponding to 40%–60% initial RDs show stiff behavior compared to the case of RD = 30%. These test results emphasize the role of the initial RD of the original ground in altering the bearing capacity after improvement.

Among the response between the untreated and treated ground, it can be inferred from Fig. 7 that all the treated cases tend to move into the nonlinear zone of deformation (plastic) between 1,200 and 1,800 kPa. One of the reasons for this behavior is, in the initial stages, the footing on the SCP-improved sand strata have undergone a gradual settlement (as seen in the initial portion of Fig. 7) while resisting the pressure applied. For increasing pressures, the footing undergoes failure with the full mobilization of friction; still offering the possible minimal resistance it could, against the failure. This *transformation zone* where the pressure–settlement plot changes from linear to nonlinear behavior is highly significant for the design of the SCP treatment technique. An ideal SCP design can be developed, where the footing can be made more stable by being in the linear part by postponing the transformation zone in the plot to occur farther behind. Although this needs a meticulous understanding of the SCP response, optimizing an SCP design based on this could be a substantial betterment when added to the existing design methodologies.

For the initial RD = 30%, the nonlinear part experienced higher settlements for lower values of the bearing pressures. For higher initial RDs, the nonlinear part of the response exhibits more stiff behavior, and also the SCP group carries higher loads with lesser settlements. Studies conducted by Bolton (1986) also noted that the failure envelope of sands can be nonlinear and the degree of nonlinearity depends on the RD and confining stress level.

SIF (η) is the ratio of the settlement of the untreated ground to that of the treated ground for the particular loaded area (McCabe and Egan 2010). The inverse of this factor is known as the settlement reduction factor (SRF) (β). The SRF plays an important role in the application of stone columns for determining the effect of improvement achieved after the treatment. Likewise, in this study, the SIF values are estimated for selected bearing pressures for all the parametric variations considered in the sensitivity analyses. To provide a better understanding of the extent of the improvement achieved by the SCP technique, these estimations are computed at 500, 1,000, and 1,500 kPa from the pressure–settlement plots. Lesser is the settlement of the treated ground, higher is the SIF (η), and vice versa (Black et al. 2011).

Fig. 8 depicts the variation of SIF with the initial RD of the sand deposit for the three bearing pressures. From the figure, it is found that the maximum improvement is achieved for the bearing pressure of 1,500 kPa for the initial RD of 60%. A linear trend is observed in SIF values for the bearing pressures of 500 and 1,000 kPa, whereas for the bearing pressure of 1,500 kPa, an exponential trend is observed. The higher values of SIF are attributed to the higher resistance offered by the treated ground, which has a higher initial RD before the treatment. It can also be noted from Fig. 7 that only at bearing pressures higher than 1,200 kPa, the improved deposit undergoes plastic deformation.

Effect of Pile Diameter

Han (2015) reported that the typical diameter of the SCPs employed in the field range from 0.6 to 0.8 m. Therefore, an adequate range of diameter of the SCP varying from 0.5 to 0.8 m is chosen in the study to assess the parametric effect on the response. The following parameters are kept constant in the analysis: initial RD = 30%, $L = 20$ m, and $S = 2D$. Fig. 9 shows the effect of the increasing diameter of the SCP on the bearing pressure–settlement ratio response of the SCP-improved sand deposit. The diameter of the SCP is varied and accordingly, the footing dimensions are obtained by the unit cell approach. For 0.5 m diameter, the footing diameter

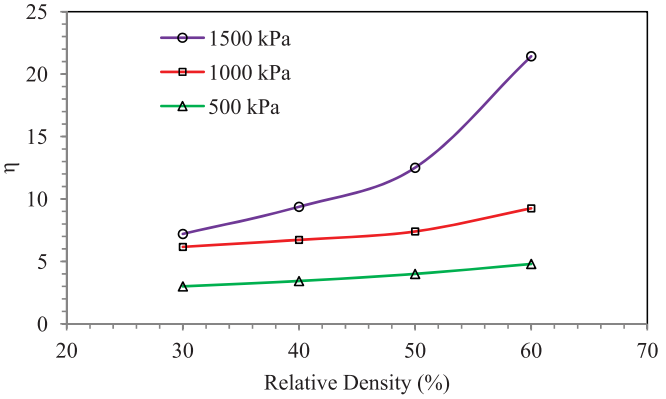

Fig. 8. Effect of the initial relative density of sand deposit on SIF (η).

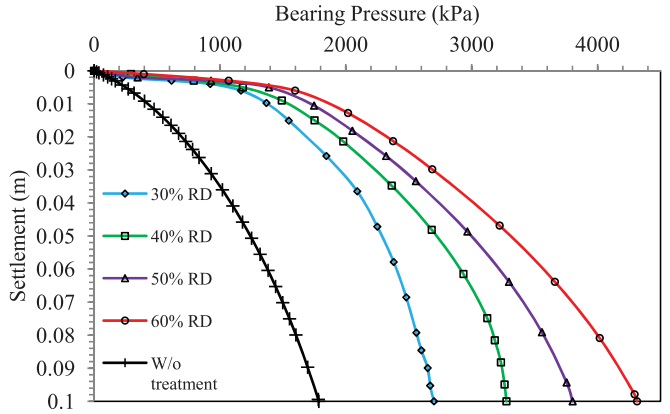

Fig. 7. Effect of initial RD on pressure–settlement response of SCP-improved sand deposit ($D = 0.6$ m, $L = 20$ m, $S = 2D$).

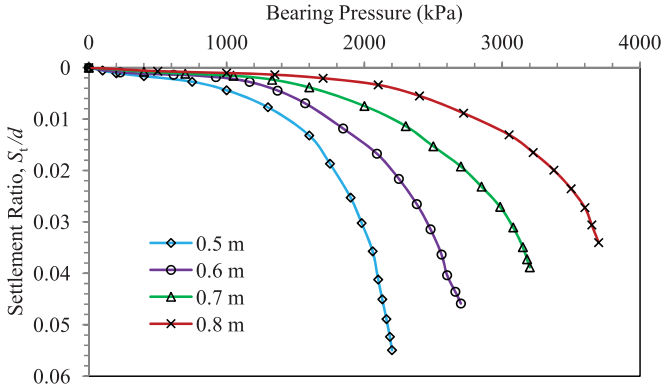

Fig. 9. Effect of SCP diameter on pressure–settlement response of footing on SCP-improved stratum (initial RD = 30%, $L = 20$ m, $S = 2D$).

(d) adopted is 1.82 m, for 0.6 m it is 2.18 m, 0.7 m it is 2.55 m, and 0.8 m it is 2.91 m. To compare the responses of the treated sand deposit with SCPs of different diameters, the settlement of the footing (S_t) is normalized with the diameter of the footing (d) for the respective cases.

For the increased diameter of the SCP (0.5–0.8 m), the trend in the response is almost linear and stiffer for the lower bearing pressures. With the increase in the bearing pressures, the pressure–settlement ratio plots (S_t/d) of the smaller diameter SCPs (i.e., 0.5 and 0.6 m) exhibit two distinct zones: the initial linear zone followed by the nonlinear inelastic one. For larger diameter SCPs (>0.7 m), the response is stiffer and the overall linear trend is observed even up to higher bearing pressures. With further increase in the bearing pressure, the response enters into the plastic zone leading to failure. It can be inferred from Fig. 9 that although the y-axis has been normalized, the *transformation zone* referred to in the previous section of the effect of initial RD exists herein too. It is to note that the transformation zone pertaining to the diameter of SCP has its range between 800 and 1,200 kPa. The reason behind the shifting of the zone to a lesser pressure range (in comparison to the previous parameter: initial RD) is due to the smaller SCP diameter (0.5 m) used. Devoid of the 0.5 m diameter SCP case, for all other cases the initial linear zone is prominent and clearly visible in Fig. 9. Therefore, it can be stated that increasing the diameter of SCP appreciably shifts the transformation zone to occur later in the pressure–settlement plots.

Based on the results, it can be stated that the larger diameter SCP increases the load-carrying capacity of the SCP-treated ground significantly, thus increasing the UBC of the footing resting on the SCP-treated ground. The increase in the UBC of the improved ground is 70% for 0.5 m diameter SCP compared to the untreated deposit. The percent increase in the bearing capacity varies from 89% to 180% for other diameters (0.6–0.8 m), as compared to the UBC of the untreated ground. Fig. 10 shows the variation of SIF (η) with the increasing diameter of the SCPs for the three selected bearing pressures. The SIF values are obtained from the pressure–settlement responses obtained from the FE analyses. From the magnitude of SIF values, it can be inferred that the 0.8 m diameter SCP provides the highest η value irrespective of the bearing pressure levels considered. This implies that for the increased diameter of the SCP, the treated ground is capable of offering higher resistance to the applied loading.

Effect of Pile Length

In the previous section, 0.8 m is the maximum diameter of the SCP adopted to study the effect of diameter on the pressure–settlement response of the treated ground. The critical lengths of granular piles recommended by Han (2015) range from 4 to 6 times the diameter of the SCP. Using this criterion for the present study, the length of the SCP corresponding to the maximum diameter (0.8 m) would result in an SCP length of 4.8 m. However, the sand deposit considered for the treatment in the study is 25 m deep. The resulting treatment with the use of SCP lengths of 4–6 times the diameter of SCP will end up improving only one-fourth of the depth from the ground level and therefore, not preferable. Also, the typical lengths of SCPs used in the field as reported again by Han (2015) vary from 5 to 15 m. Thus, the lengths of the SCPs considered in the study include the critical lengths and typical lengths used in practice to assess the extent of improvement.

The length of the SCPs is varied as follows: 2.4, 3, 3.6, 5, 10, 15, and 20 m in the analysis. The maximum length of the SCP chosen is 20 m leaving 5 m from the bottom of the FE domain to avoid boundary effects if any. The other parameters are kept as constant: initial RD = 30%, $D = 0.6$ m, and $S = 2D$. The pressure–settlement response obtained from the FE analysis (Fig. 11) depicts that stiff behavior is exhibited by the treated ground for higher lengths of the SCPs. It is noted that the SCP length greater than 5 m, which is higher than $6D$, resulted in a better load-carrying capacity of the treated ground. It can be inferred from Fig. 11 that, lesser is the length of the SCP, the occurrence of transformation zone is highly unlikely. One of the reasons for this behavior is the lesser magnitude of frictional resistance offered by the SCPs against the movement of the footing. Also, it can be clearly seen that 15 and 20 m lengths of SCPs are found to have the *transformation zone*, in the pressure range between 600 and 1,200 kPa.

The pressure–settlement plots obtained from the typical lengths are only considered for the evaluation of SIF values since these lengths of SCPs are more promising in terms of efficiency in the improvement of the sand deposit. Fig. 12 depicts the variation of SIFs with different lengths of the SCPs for the three selected bearing pressures. Among the lengths used, the length of SCP = 20 m achieves the highest SIF values (4–9.25). Therefore, it can be stated that by adopting the increased lengths for SCPs, it is possible to obtain better performance from the treated ground.

In comparison with the percent increment in UBC for different SCP lengths, the increasing diameter of SCP for a particular length provides a higher enhancement in the strength characteristics of the treated ground. This implies that the use of larger diameter for the SCP is beneficial concerning the strength enhancement of the treated ground. Among the choices available with the designer, for economic considerations, increasing the diameter of the SCP by 100 mm enhances the UBC of the treated ground by more than 20% for the same length of the SCP. This way one can handle

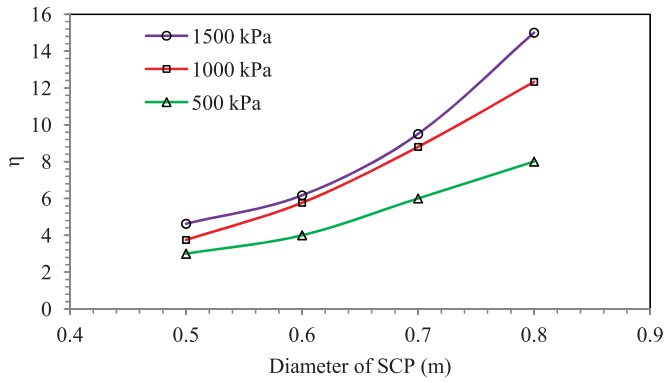

Fig. 10. Effect of the diameter of SCP on SIF (η).

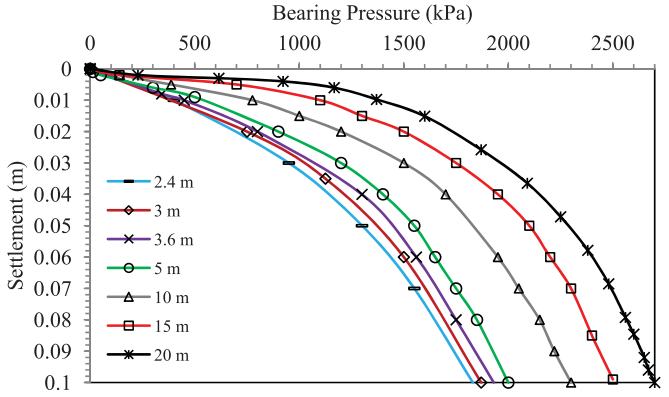

Fig. 11. Effect of SCP length on pressure–settlement response of SCP-improved deposit (initial RD = 30%, $D = 0.6$ m, $S = 2D$).

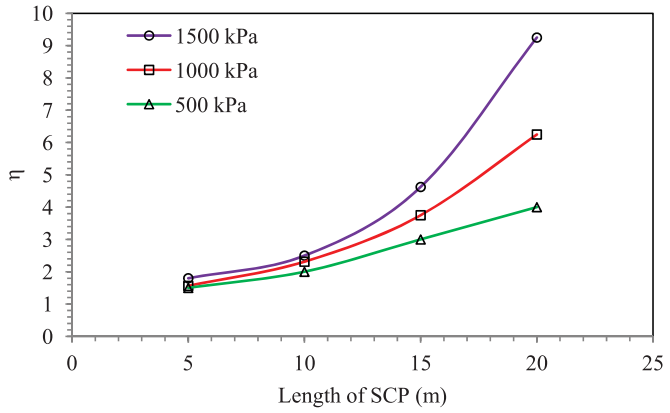

Fig. 12. Effect of length of SCP on SIF (η).

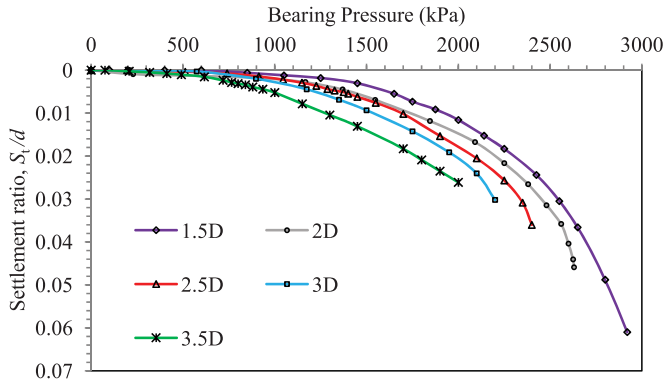

Fig. 13. Effect of spacing on pressure–settlement ratio response of footing resting on SCP-improved sand deposit (initial RD = 30%, $D = 0.6$ m, $L = 20$ m).

the uncertainties associated with the properties of the sand deposit reliably. Further studies are needed in this regard to examine the other possibilities for the critical lengths and accordingly, the recommendations can be made available.

Effect of Spacing

The effect of spacing of SCP on the load-carrying capacity of the SCP-improved sand deposit is studied by varying the spacing from 1.5 to 3.5D. The other parameters are kept constant during the analysis: initial RD = 30%, $D = 0.6$ m, and $L = 20$ m. The footing dimensions used for 1.5D spacing is 1.64 m, 2D spacing is 2.18 m, 2.5D spacing is 2.74 m, 3D spacing is 3.28 m, and 3.5D spacing is 3.83 m. The settlement of the footing is normalized with the diameter of the footing, which is a function of the SCP spacing. From Fig. 13, it can be noted that when the spacing increases, the pressure–settlement ratio plot exhibits less stiff behavior. For lower bearing pressures, the response is almost the same for all the spacings. At higher bearing pressures, the pressure–settlement ratio plot corresponding to the smaller spacing exhibits higher stiffness, as well as more nonlinearity. It is concluded that for the higher spacing of the SCPs, lesser is the UBC of the SCP group and vice versa. Fig. 13 shows the SCPs, even though installed over a wider spacing range, the initial linear portion extends up to a pressure range of 700 kPa. The *transformation zone* based on the parameter of spacing is occurring between 700 and 1,700 kPa. This transformation zone for the considered spacing

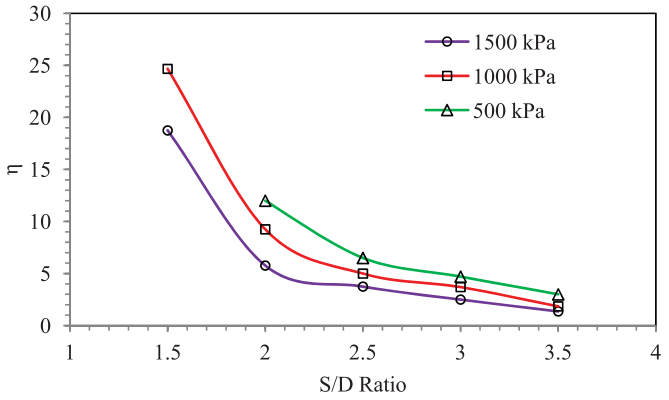

Fig. 14. Effect of pile spacing adopted on SIF (η).

range in the present study exists over a larger pressure range and is highly preferable in the design of the SCP technique for a site.

Fig. 14 shows the effect of varying pile spacing on the SIF (η) evaluated by the pressure–settlement responses. Similar to the previous cases, the SIF values obtained from the pressure–settlement plot corresponding to the bearing pressures of 1,000 and 1,500 kPa resulted in much higher values for the lesser spacing of the SCPs. Independent of the bearing pressures considered, the spacing of 1.5D provides the best results concerning the SIF. It is noted that for the field-scale problem, the spacing of 1.5D yields the maximum improvement in terms of the UBC of the treated ground.

Conclusions

The efficiency of the SCPs in improving the loose to medium dense sand deposits is investigated by performing 3D FE simulations. The laboratory-scale SCP model is simulated using the finite-element method (FEM) and is validated with the experimental result. The validated FE model is extended to the field-scale dimensions and the parametric sensitivity analyses are performed. The influence of material and geometric properties of the sand deposit and the SCPs on the pressure–settlement response of the SCP-treated deposit is studied in detail. The following are the conclusions from the present study:

- For the field-scale model, the footing resting on the SCP-improved sand deposit with initial RD > 50% undergoes failure for the displacement of 0.1 m. It is to note, the failure in the nonlinear zone is gradual and the pressure–settlement plot is more toward the x-axis in comparison to smaller initial RDs. This is due to the higher densification and increased stiffness offered by the SCP group after the improvement.
- Increasing the diameter of SCP increases the load-carrying capacity of the SCP-treated sand deposits in comparison to an increase in SCP length. Herein the study, increasing the diameter of the SCP by 100 mm enhances the UBC of the treated ground by more than 20% for the same length of the SCP.
- For the SCP group, lengths greater than 8D achieves the better load-carrying capacity of the treated ground. This is due to the increase in frictional resistance offered by the group along the periphery of the shaft when larger lengths are considered in the FE simulations.
- The failure trend of the SCP-improved deposit need not be necessarily always nonlinear. It is highly dependent on the range of spacing adopted. For example, in the present study, footing resting on SCP installed for higher spacing (e.g., 3.5D) undergoes

Int. J. Geomech., 2021, 21(4): 04021019

failure under loading. However, the pressure–settlement ratio plot obtained is found to be more linear in comparison to the smaller spacing (e.g., 1.5D) studied.
- The SIF of the treated ground provides valuable information on the degree of improvement achieved for the deposit. These factors are mainly dependent on the spacing of the SCPs and the initial relative density of the deposit.

Data Availability Statement

All data, models, and codes generated or used during the study appear in the published article.

Acknowledgments

The authors wish to thank Dr. B. R. Madhusudhan for his valuable suggestions during the preparation of the manuscript. Help rendered by the Head, Department of Ocean Engineering at the Indian Institute of Technology Madras, Chennai with using PLAXIS 3D software is deeply acknowledged.

Notation

The following symbols are used in this paper:

D = diameter of the SCP;
d = diameter of the footing;
E = Young's modulus;
L = length of the SCP;
R_{inter} = interface reduction factor;
r_e = relative element size factor;
S/D = ratio of spacing between the SCP/diameter of the SCP;
S_t = settlement of the footing;
S_t/d = settlement ratio;
U_x = displacement in the x-direction;
U_y = displacement in the y-direction;
U_z = displacement in the z-direction;
β = settlement reduction factor;
γ = unit weight;
η = settlement improvement factor;
υ = Poisson's ratio;
ϕ = internal angle of friction; and
ψ = dilatancy angle.

References

Aarthi, N., A. Boominathan, and S. R. Gandhi. 2019. "Experimental study on the behaviour of sand compaction columns in sandy strata." *Int. J. Geotech. Eng.* 1–14. https://doi.org/10.1080/19386362.2019.1710391.

Aboshi, H., E. Ichimoto, M. Enoki, and K. Harada. 1979. "The composer—A method to improve characteristics of soft clays by inclusions of large diameter sand columns." In Vol. 1 of *Int. Conf. Soil Reinforcement: Reinforced Earth and Other Techniques*, 211–216. Paris, France: Np.

Ambily, A. P., and S. R. Gandhi. 2007. "Behaviour of stone columns based on experimental and FEM analysis." *J. Geotech. Geoenviron. Eng.* 133 (4): 405–415. https://doi.org/10.1061/(ASCE)1090-0241(2007)133:4(405).

Ammari, K. A., and B. G. Clarke. 2018. "Effect of vibro stone-column installation on the performance of reinforced soil." *J. Geotech. Geoenviron. Eng.* 144 (9): 04018056. https://doi.org/10.1061/(ASCE)GT.1943-5606.0001914.

Ashwathy, M. S., M. Bala Subramanian, N. Sugavaneswaran, and V. Jayapragash. 2013. "Performance of sand compaction piles in sandy silt." In Vol. 1 of *Indian Geotechnical Conf.*, 1–4. Roorkee, India: IIT Roorkee.

ASTM. 2011. *Standard test method for direct shear test of soils under consolidated drained conditions*. ASTM D3080/D3080M-11. West Conshohocken, PA: ASTM.

ASTM. 2016. *Standard test method for nonrepetitive static plate load tests of soils and flexible pavement components, for use in evaluation and design of airport and highway pavements*. ASTM D1196/D1196M-12. West Conshohocken, PA: ASTM.

Basack, S., and R. D. Purkayastha. 2009. "Engineering properties of marine clays from the eastern coast of India." *J. Eng. Technol. Res.* 1 (6): 109–114. https://doi.org/10.5897/JETR.9000038.

Basack, S., F. Siahaan, B. Indraratna, and C. Rujikiatkamjorn. 2018. "Stone column–stabilized soft-soil performance influenced by clogging and lateral deformation: Laboratory and numerical evaluation." *Int. J. Geomech.* 18 (6): 04018058. https://doi.org/10.1061/(ASCE)GM.1943-5622.0001148.

Bhowmik, R., and M. Samanta. 2013. "Numerical analysis of piled-raft foundation under vertical load in stone column improved soil." In *Indian Geotechnical Conf.*, 1–10. Roorkee, India: IIT Roorkee.

BIS (Bureau of Indian Standards). 1992. *Indian standard code of practice guidelines for selection of ground improvement techniques for foundation in weak soils*. IS 13094-1992. New Delhi, India: BIS.

Black, J. A., V. Sivakumar, and A. Bell. 2011. "The settlement performance of stone column foundations." *Géotechnique* 61 (11): 909–922. https://doi.org/10.1680/geot.9.P.014.

Bolton, M. D. 1986. "The strength and dilatancy of sands." *Géotechnique* 36 (1): 65–78. https://doi.org/10.1680/geot.1986.36.1.65.

Bouassida, M., and J. P. Carter. 2014. "Optimization of design of column-reinforced foundations." *Int. J. Geomech.* 14 (6): 04014031. https://doi.org/10.1061/(ASCE)GM.1943-5622.0000384.

Bowles, J. E. 1996. *Foundation analysis and design*. New York: McGraw-Hill.

Briaud, J. L., and R. M. Gibbens. 1994. "Predicted and measured behavior of five spread footings on sand." In *Federal Highway Administration at the 1994 American Society of Civil Engineers, Conf. Settlement'94*, 192–218. Reston, VA: ASCE.

Broere, W., and A. F. van Tol. 2006. "Modelling the bearing capacity of displacement piles in sand." *Proc. Inst. Civ. Eng. Geotech. Eng.* 159 (3): 195–206. https://doi.org/10.1680/geng.2006.159.3.195.

Carter, J. P., C. S. Desai, D. M. Potts, H. F. Schweiger, and S. W. Sloan. 2000. "Computing and computer modelling in geotechnical engineering." In *GeoEng 2000, Int. Conf. on Geotechnical and Geological Engineering*, 1157–1252. Lancaster, PA: Technomic.

Chen, Q., and M. A. Farsakh. 2011. "Numerical analysis to study the scale effect of shallow foundation in reinforced soils." In *Geo-Frontiers 2011: Advances in Geotechnical Engineering*, Geotechnical Special Publication 221, edited by J. Han, and D. E. Alzamora, 595–604. Reston, VA: ASCE.

Coombs, W. M., R. S. Crouch, and C. E. Heaney. 2013. "Observations on Mohr–Coulomb plasticity under plane strain." *J. Eng. Mech.* 139 (9): 1218–1228. https://doi.org/10.1061/(ASCE)EM.1943-7889.0000568.

Damians, I. P., R. J. Bathurst, A. Josa, and A. Lloret. 2015. "Numerical analysis of an instrumented steel-reinforced soil wall." *Int. J. Geomech.* 15 (1): 04014037. https://doi.org/10.1061/(ASCE)GM.1943-5622.0000394.

Dixit, M. 2016. "Damage mechanism in problematic soils." *Int. J. Civ. Eng. Technol.* 7 (5): 232–241.

Fellenius, B. H., and A. Altaee. 1994. "Stress and settlement of footings in sand." In Vol. 2 of *Vertical and Horizontal Deformations for Foundations and Embankments*, Geotechnical Special Publication 40, 1760–1773. Reston, VA: ASCE.

Han, J. 2015. *Principles and practice of ground improvement*. Hoboken, NJ: Wiley.

Hanna, A. M., M. Etezad, and T. Ayadat. 2013. "Mode of failure of a group of stone columns in soft soil." *Int. J. Geomech.* 13 (1): 87–96. https://doi.org/10.1061/(ASCE)GM.1943-5622.0000175.

Harada, K., M. Yamamoto, and J. Ohbayashi. 1998. "On ko value of improved ground by static compaction technique." In *Proc., 53rd Annual Conf. of the Japan Society of Civil Engineers*, 544–545. Tokyo: JSCE.

Hatanaka, M., L. Feng, N. Matsumura, and H. Yasu. 2008. "A study on the engineering properties of sand improved by the sand compaction pile method." *Soils Found.*. 48 (1): 73–85. https://doi.org/10.3208/sandf.48.73.

Hirao, H., and M. Matsuo. 1985. "Study on upheavad ground generated by sand compaction piles." *Doboku Gakkai Ronbunshu.* 364: 169–178. https://doi.org/10.2208/jscej.1985.364_169.

Hurley, O., M. Nuth, and M. Karray. 2015. "Finite element modeling of stone column installation: Review of modelling and case study with PLAXIS 2D." In *GEOQuebec*, 1–8. Canada: Canadian Geotechnical Society (CGS).

Jeludin, D. K. N. M. PG. H., V. Sivakumar, B. C. O. Kelly, and P. A. Mackinnon. 2016. "Experimental observations of settlement of footings supported on soft clay reinforced with granular columns: Laboratory model study." *J. Geotech. Geoenviron. Eng.* 142 (1): 04015063. https://doi.org/10.1061/(ASCE)GT.1943-5606.0001377.

Jozefiak, K., A. Zbiciak, M. Maslakowski, and T. Piotrowski. 2015. "Numerical modelling and bearing capacity analysis of pile foundation." *Procedia Eng.* 111: 356–363. https://doi.org/10.1016/j.proeng.2015.07.101.

Kankara, R. S., M. V. Ramana Murthy, and M. Rajeevan. 2018. *National assessment of shoreline changes along Indian coast—A status report for 1990–2016*. Chennai, India: NCCR.

Kinoshita, H., K. Harada, M. Nozu, and J. Ohbahayshi. 2012. "Sand compaction pile technology and its performance in both sandy and clayey grounds." In *Int. Symp. on Ground Improvement*, 1–10. London, UK: ISSMGE TC211.

Kitazume, M., A. Takahashi, K. Harada, and N. Shinkawa. 2016. "New type sand compaction pile method for densification of liquefiable ground underneath existing structure." *J. Geo-Eng. Sci.* 3 (1): 1–13. https://doi.org/10.3233/JGS-150032.

Kranthikumar, A., V. A. Sawant, P. Kumar, and S. K. Shukla. 2016. "Numerical and experimental investigations of granular anchor piles in loose sandy soil subjected to uplift loading." *Int. J. Geomech.* 17 (2): 04016059. https://doi.org/10.1061/(ASCE)GM.1943-5622.0000733.

Lozovyi, S., and E. Zahouriko. 2012. "PLAXIS simulation of static pile tests and determination of reaction piles influence." *Sci. Tech. J.: New Technol. Constr.* 23–24 (1–2): 68–73.

Madhusudhan B. R., A. Boominathan, and S. Banerjee. 2019. "Engineering properties of sand–rubber tire shred mixtures." *Int. J. Geotech. Eng.* 1–7. https://doi.org/10.1080/19386362.2019.1617479.

McCabe, B., and D. Egan. 2010. "A review of the settlement of stone columns in compressible soils." In *Ground Improvement and Geosynthetics*, Geotechnical Special Publication 207, edited by A. J. Puppala, J. Huang, J. Han, and L. R. Hoyos, 197–204. Reston, VA: ASCE.

Moh, Z. C., C. D. Ou, S. M. Woo, and K. Yu. 1981. "Compacted sand piles for soil improvement." In Vol. 3 of *Proc., 10th Int. Conf. on Soil Mechanics and Foundation Engineering*, 749–752. Rotterdam, The Netherlands: A.A. Balkema

Nyström, M., and V. Persson. 2016. "Soil displacement due to piling." M.S. thesis, Dept. of Civil and Environmental Engineering, Chalmers Univ. of Technology.

Raj, D., and C. V. Dikshith. 2010. "Vibro replacement columns for shipyard infrastructure at Pipavav, Gujarat, India." In *Int. Symp. on Ground Improvement Technologies and Case Histories*, 763–769. Singapore: GeoSS.

Samanta, M., V. A. Sawant, and G. Ramasamy. 2010. "Ground improvement using displacement type sand piles." In *Indian Geotech. Conf.—GeoTrendz*, 629–632, Mumbai, India: IIT Bombay.

Savidis, S. A., F. Rackwitz, and M. Schubler. 2008. "Design and construction of granular columns for ground improvement of very soft soils for road embankments." In *Proc., 6th Int. Conf. on Case Histories in Geotechnical Engineering*, 1–11. Rolla, MO: Missouri Univ. of Science and Technology.

Shiomi, M., and K. Kawamoto. 1986. "Prediction of ground heave associated with the installation of sand compaction piles." In *Proc., 21st Annual Conf. of the Japanese Society of Soil Mechanics and Foundation Engineering*, 1861–1862. Japan: Np.

Singh, R., D. Roy, and S. K. Jain. 2005. "Analysis of earth dams affected by the 2001 Bhuj earthquake." *Eng. Geol.* 80 (3–4): 282–291. https://doi.org/10.1016/j.enggeo.2005.06.002.

Sogabe, T. 1981. "Technical subjects on design and execution of sand compaction pile method." In Vol. 3 of *Proc., 36th Annual Conf. Japan Society of Civil Engineers*, 39–50, Tokyo: JSCE.

Takeuchi, H., T. Noda, and A. Asaoka. 2010. "Numerical analysis on co- and postseismic behavior of sandy/clayey soil ground improved by sand compaction pile method." In *Soil Dynamics and Earthquake Engineering*, Geotechnical Special Publication 201, edited by M. Huang, X. Yu, and Y. Huang, 218–224. Reston, VA: ASCE.

Uppal, H. L., and L. R. Chadda. 1967. "Physico-chemical changes in the lime stabilization of black cotton soil (India)." *Eng. Geol.* 2 (3): 179–189. https://doi.org/10.1016/0013-7952(67)90017-8.

Vermeer, P. A., and R. B. J. Brinkgreve. 2013. *PLAXIS 3d user's manual*. Rotterdam, Netherlands: A. A. Balkema.

Wei, J. 1997. "Ground improvement techniques—The HDB way." In *Int. Conf. Ground Improvement Techniques*. 609–620. Singapore: CI-Premier Pte Ltd.

White, D., and M. D. Bolton. 2002. "Soil deformation around a displacement pile in sand." In Vol. 1 of *Int. Conf. Physical Modeling in Geotechnics: ICPMG 02*, edited by R. Philips, P. J. Guo, and R. Popescu, 649–654. Rotterdam, Netherlands: Balkema.

Yabushita, H., M. Terada, and N. Suematsu. 1973. "Compulsory replacement method of soft clay ground." *J. Jpn. Soc. Soil Mech. Found. Eng.* 21 (9): 33–40.

Yamamoto, M., K. Harada, M. Nozu, and J. Ohbayashi. 1997. "Study on evaluation of increasing density due to penetrating sand piles." In *Proc., 32nd Annual Conf. Japanese Society of Soil Mechanics and Geotechnical Engineering*, 2631–2632. Tokyo: JSCE.

Yasuda, S., K. Ishihara, K. Harada, and N. Shinkawa. 1996. "Effect of soil improvement on ground subsidence due to liquefaction." *Soils Found.* 36: 99–107. https://doi.org/10.3208/sandf.36.Special_99.

Yi, J. T., S. H. Goh, and F. H. Lee. 2013. "Effect of sand compaction pile installation on strength of soft clay." *Géotechnique* 63 (12): 1029–1041. https://doi.org/10.1680/geot.12.P.108.